Comparison of Reconstruction Strategies of Compressive Sensing Applied to Ultrasound Images

Erick Toledo Gómez(✉), Humberto de Jesús Ochoa Domínguez,
Soledad Vianey Torres Argüelles,
and Leandro José Rodríguez Hernández

Departamento de Ingeniería Industrial y Manufactura,
Universidad Autónoma de Ciudad Juárez, Ciudad Juárez, Mexico
etg.pds@gmail.com

Abstract. Ultrasound medical images are important for medical diagnose. The method allows the real-time visualization of organs of the body and it is not invasive. In this study, a comparison of reconstruction greedy search methods, used in compressive sensing, is performed. The methods and the algorithms are explained and experiments are carried out in synthetic and measured data. Result show that the orthogonal matching pursuit outperforms the other methods in the greedy search classification.

Keywords: Compressive sensing · Sampling matrix · Sparsity
Ultrasound images

1 Introduction

Medical images are important for the diagnose of human beings. An important area of study is the ultrasound (US) images, which have the special feature of being captured in real time. The ultrasound signals are acquired through a transducer that sends ultrasonic waves at a frequency higher than 20 kHz [1], spreading across of the body, until colliding with the soft tissues which causes the wave to be reflected.

The compressive sensing (CS) area integrates different stages such as sampling, reduction of the dimensionality, compression and optimization, and it has been used to introduce improvements in the reconstruction of these images. The CS [2–4] aims at reconstructing signals by a number of measures significantly lower than the necessary when using the Shannon/Nyquist sampling theory [5, 6]. To apply the CS to signals, a fundamental property called sparseness [7, 8] must be fulfilled.

The reconstruction of the US image is usually computationally expensive, hence, the reconstruction algorithms are an important step in CS. These algorithms are divided into five groups: Bayesian methods, convex relaxation, greedy search, non-convex relaxation and brute force [9]. In this paper, a comparison of greedy algorithms for reconstructing US images is performed. The metrics used are the structural similarity index (SSIM), which is a quality metric for measuring the similarity between the original and the recovered images and peak signal to noise ratio (PSNR).

© Springer Nature Switzerland AG 2019
T. Antipova and A. Rocha (Eds.): DSIC 2018, AISC 850, pp. 456–464, 2019.
https://doi.org/10.1007/978-3-030-02351-5_52

The paper is organized as follows: Sect. 2 presents the conditions that must be met both the measurement vector and the sampling matrix to be able to apply the CS. In Sect. 3, the greedy algorithms (OMP, CoSaMP, HTP and IHT [10–13]) are explained. Section 4 provides the results of the algorithms when retrieving the US images in simulated data. Section 5 provides the results of measured data. The paper concludes in Sect. 6.

2 Compressive Sensing

The goal of CS is to reconstruct a vector $\boldsymbol{x} \in \mathbb{R}^N$ that satisfies the linear equation $\boldsymbol{y} = \boldsymbol{\Phi x}$, where $\boldsymbol{\Phi} \in \mathbb{R}^{MxN}$ is the sensing matrix and the vector $\boldsymbol{y} \in \mathbb{R}^M$ has a reduction of dimensionality with respect to the input sparse vector $\boldsymbol{x} \in \mathbb{R}^N$, that is M $\ll$ N.

Sparsity property allows to obtain compressed samples, which can be reconstructed with precision [7, 8]. A signal is sparse if it has only a few non-zero coefficients, compared to the signal length, for a vector $\boldsymbol{x} \in \mathbb{R}^N$ the sparsity can be expressed as follows:

$$\|\boldsymbol{x}\|_0 \leq k. \tag{1}$$

A sparse vector $\boldsymbol{x} \in \mathbb{R}^N$ can be represented through with a linear combination of few coefficients of a known base or dictionary $\boldsymbol{\Psi}$. If this representation is exact then the signal is sparse.

$$x_i = \sum_{i=1}^{n} z_i \psi_i \quad \Rightarrow \quad \boldsymbol{x} = \boldsymbol{\Psi z} \quad \text{with} \quad \|z\|_0 \leq k. \tag{2}$$

$\boldsymbol{\Psi}$ is an array of N $\times$ N with $[\psi_1, \psi_2, \ldots \psi_N]$ column vectors and z_i the sequence of coefficients of $\boldsymbol{x}$ [14]. The sparse signals can be recovered using CS if they have been contaminated with noise $\boldsymbol{y} = \boldsymbol{\Phi x} + \boldsymbol{\eta}$, where $\boldsymbol{\eta}$ is the noise component. In order to reconstruct the signal the Restricted Isometry Property (RIP) [8, 14] must fulfilled.

Theorem 1 [8]. *If for any positive number L there exists a Constant Restricted Isometry (RIC)* $\delta_L \in (0, 1)$, *it is said that the matrix* $\boldsymbol{\Phi}$ *satisfies the L-order RIP, in other words*,

$$(1 - \delta_L)\|\boldsymbol{x}\|_2^2 \leq \|\boldsymbol{\Phi x}\|_2^2 \leq (1 + \delta_L)\|\boldsymbol{x}\|_2^2 \quad \textit{for all } \boldsymbol{x} \textit{ such that} \quad \|\boldsymbol{x}\|_0 \leq L. \tag{3}$$

If $\boldsymbol{\Phi} \in \mathbb{R}^{MxN}$ satisfies RIP of order $2k$ implies that the distances between all vectors k-sparse are preserved. Then, the sampling matrix assign a single vector k-sparse at the same point. To recover any sparse signal $\boldsymbol{x} \in \mathbb{R}^N$, that satisfies $\boldsymbol{y} = \boldsymbol{\Phi x}$ with $\boldsymbol{\Phi} \in \mathbb{R}^{MxN}$, $\boldsymbol{y} \in \mathbb{R}^M$ and M $\ll$ N it is required to solve the following optimization problem,

$$min \ \|\boldsymbol{x}\|_0 \quad s.t \quad \boldsymbol{\Phi x} = \boldsymbol{y}. \tag{4}$$

When the signal is contaminated with noise, the model of the signal becomes $\boldsymbol{y} = \boldsymbol{\Phi x} + \boldsymbol{\eta}$ and the optimization problem changes to solve,

$$min \ \|\boldsymbol{x}\|_0 \quad s.t \quad \|\boldsymbol{y} - \boldsymbol{\Phi x}\|_2 \leq \sigma_n^2. \tag{5}$$

where σ_n^2 is a measure of the power of the noise. For the two cases of optimization problems to solve previously mentioned with the l_0, they are algorithms of the type NP-HARD [15]. That is, solving this type of algorithms for any measurement matrix $\boldsymbol{\Phi}$ is computationally intractable.

3 Greedy Search Algorithms

Greedy algorithms present a simple analysis and low complexity [16]. In these algorithms for each iteration the residue vector is calculated from the projection of the sparse vector on the sampling matrix ($\boldsymbol{\Phi}$), until the stopping condition is satisfied, throwing an approximation to the original vector as output. Within this group are the Orthogonal Matching Pursuit (OMP) [10] and the Compressive Sampling Matching Pursuit (CoSaMP) [11]. Algorithms based on threshold methods are another variety that give us an approximation to the original vector, among them give the Iterative Hard Thresholding (IHT) [13] and Hard Thresholding Pursuit (HTP) [12]. The following algorithms are used to find the solution of (6).

$$\boldsymbol{x}^* = argmin \ \|\boldsymbol{x}\|_0 \quad s.t \quad \|\boldsymbol{y} - \boldsymbol{\Phi x}\|_2 \leq \sigma_n^2. \tag{6}$$

3.1 Orthogonal Matching Pursuit (OMP)

The OMP is characterized by its simplicity and high speed [10]. The algorithm initializes a residual vector $\boldsymbol{r}$ equal to the vector $\boldsymbol{y}$ and in each iteration the function is orthogonally projected on all the vectors that have been selected from the sampling matrix, until the stop condition is met, resulting in an approximation to the original vector. The Algorithm 1 implements the OMP.

3.2 Compressive Sampling Matching Pursuit (CoSaMP)

In each iteration, the indices of the $2k$-sparse vectors for which the correlation between the sampling matrix and the residual is maximum. Subsequently, the minimum square is searched using the selected vectors of the sampling matrix. Leaving only the k largest components of this solution and updating the residual vector. When the stopping conditions are met, an approximation to the original vector is obtained. The Algorithm 2 implements the CoSaMP.

The non-linear operator $H_k(*)$ is a hard thresholding of order k which retains the k highest absolute values of $\boldsymbol{x}$ and makes zero the remaining.

Algorithm 1 : Orthogonal Matching Pursuit (OMP)

In: Φ , y , σ_η^2
Initialize: $r \leftarrow y$; $\Omega \leftarrow \varnothing$; $j \leftarrow 0$; $i \leftarrow 0$; $x^* \leftarrow \varnothing$
while $\|r\|_2^2 > \sigma_\eta^2$ **do**
  $x_j \leftarrow \phi_j^T r$ for all $j \notin \Omega$
  $i \leftarrow \underset{j \notin \Omega}{argmax} |x_j|$
  $\Omega \leftarrow \Omega \cup i$
  $x_\Omega^* \leftarrow \underset{x}{argmin} \|\Phi_\Omega x - y\|_2^2$
  $r \leftarrow y - \Phi_\Omega x_\Omega^*$
  $j \leftarrow j + 1$
end while
Out: x^*

Algorithm 2 : Compressive Sampling Matching Pursuit (CoSaMP)

In: Φ , y , k , σ_η^2
Initialize: $r \leftarrow y$; $\Omega \leftarrow \varnothing$; $j \leftarrow 0$; $S \leftarrow \varnothing$; $x \leftarrow \varnothing$
while $\|r\|_2^2 > \sigma_\eta^2$ **do**
  $\Omega_{j+1} \leftarrow supp(H_{2k}(\Phi^T r_j))$
  $S_{j+1} \leftarrow \Omega_{j+1} \cup supp(x_j)$
  $\widetilde{x}_{j+1} \leftarrow \underset{x}{argmin} \left\|\Phi_{S_{j+1}} x - y\right\|_2^2$
  $(\widetilde{x}_{j+1})_i \leftarrow 0 \; for \; all \; i \notin S_{j+1}$
  $x_{j+1} \leftarrow H_k(\widetilde{x}_{j+1})$
  $r_{j+1} \leftarrow y - \Phi x_{j+1}$;
  $j \leftarrow j + 1$
end while
Out: $x^* \leftarrow x_{j+1}$

3.3 Iterative Hard Thresholding (IHT)

Thresholding algorithms use the operator $H_k(*)$ to maintain the k highest absolute values of $\boldsymbol{x} \in \mathbb{R}^N$. In each iteration, a better approximation to the vector k-sparse is sought through the Eq. (7). Where the residue vector is projected onto the sampling matrix and added to the approximation of the previous iteration and then only the k higher absolute values of the solution thrown are maintained [17]. The Algorithm 3 implements the IHT.

$$\boldsymbol{x}_{n+1} = H_k\left(\boldsymbol{x}_n + \boldsymbol{\Phi}^T(\boldsymbol{y} - \boldsymbol{\Phi}\boldsymbol{x}_n)\right). \tag{7}$$

3.4 Hard Thresholding Pursuit (HTP)

In each iteration the residue vector is projected on the sampling matrix, the result added to the approximation of the previous iteration and the supreme of the k highest absolute

values obtained is sought. Solving a minimum square taking only the selected vectors columns of the sampling matrix [18]. The Algorithm 4 implements the HTP.

Algorithm 3 : Iterative Hard Thresholding (IHT)

In: Φ , y , k , σ_η^2
Initialize: $r_0 \leftarrow y$; $d_0 \leftarrow \varnothing$; $j \leftarrow 0$; $x_0 \leftarrow \varnothing$
while $\|r\|_2^2 > \sigma_\eta^2$ **do**
$d_{j+1} \leftarrow x_j + \Phi^T r_j$
$x_{j+1} \leftarrow H_k(d_{j+1})$
$r_{j+1} \leftarrow y - \Phi x_{j+1}$
$j \leftarrow j + 1$
end while
Out: $x^* \leftarrow x_{j+1}$

Algorithm 4 : Hard Thresholding Pursuit (HTP)

In: Φ , y , k , σ_η^2
Initialize: $r_0 \leftarrow y$; $d_0 \leftarrow \varnothing$;$j \leftarrow 0$; $x_0 \leftarrow \varnothing$; $S \leftarrow \varnothing$
while $\|r\|_2^2 > \sigma_\eta^2$ **do**
$d_{j+1} \leftarrow x_j + \Phi^T r_j$
$S_{j+1} \leftarrow supp(H_k(d_{j+1}))$
$x_{j+1} \leftarrow \underset{x}{argmin} \left\|\Phi_{S_{j+1}} x - y\right\|_2^2$
$(x_{j+1})_i \leftarrow 0 \; for \; all \; i \notin S_{j+1}$
$r_{j+1} \leftarrow y - \Phi x_{j+1}$
$j \leftarrow j + 1$
end while
Out: $x^* \leftarrow x_{j+1}$

Table 1 shows the RIC conditions a be fulfilled [19] for the strategy tested.

Table 1. RIC conditions for the different algorithms [19].

OMP	CoSaMP	HTP	IHT
$\delta_{13K} < 0.1666$	$\delta_{4K} < 0.4782$	$\delta_{3K} < 0.5773$	$\delta_{3K} < 0.5773$

4 Results of Synthetic Data

In this investigation, the image of US of a phantom of cysts [20] was used. The image was divided into blocks of 8 × 8 samples and the orthonormal basis of the discrete cosine transform (DCT) was used to obtain the sparse vector. The results show that as we take fewer samples it becomes more difficult to obtain a reconstructed image similar to the original one.

Table 2 shows the quantitative results of the cyst phantom. The performance of the algorithms was measured using the Structural Similarity Index Metric (SSIM) and the Peak Signal to Noise Ratio (PSNR).

Table 2. Results of the simulation using the cyst phantom [20].

Transformed	Algorithm	(%) Coefficients	SSIM	PSNR
DCT-II	OMP	15.63	**0.92063**	**31.1298**
DCT-II	CoSaMP	15.63	0.53382	20.2263
DCT-II	HTP	15.63	0.62673	23.8842
DCT-II	IHT	15.63	0.62660	23.8387
DCT-II	OMP	31.5	**0.98245**	**36.3830**
DCT-II	CoSaMP	31.5	0.74486	24.9654
DCT-II	HTP	31.5	0.87370	28.9667
DCT-II	IHT	31.5	0.87362	28.9565
DCT-II	OMP	50	**0.99847**	**46.1240**
DCT-II	CoSaMP	50	0.84211	27.5830
DCT-II	HTP	50	0.84633	27.9177
DCT-II	IHT	50	0.84606	27.9021

Figure 1 shows the original and recovered cyst phantom image. Notice that visually, the recovered images with CoSaMP (Fig. 1(b) and (g)) have dark point that are not part of the original image.

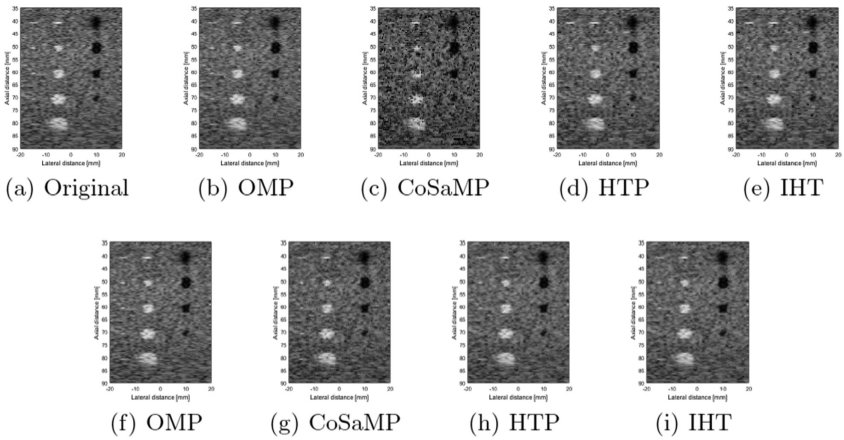

Fig. 1. Synthetic US images (a) original cyst phantom [20] and reconstructed phantoms with k = 4 and 15.6% of coefficients using (b) OMP, (c) CoSaMP, (d) HTP, (e) IHT, k = 15 and 50% of coefficients using (f) OMP, (g) CoSaMP, (h) HTP and (i) IHT.

5 Results of Measured Data

Tests on measured data were performed under the same test conditions as used in the cyst phantom [20]. Table 3 shows the quantitative results using measured data.

Table 3. Results with real US image

Transformed	Algorithm	(%) Coefficients	SSIM	PSNR
DCT-II	OMP	15.63	**0.77571**	**25.5944**
DCT-II	CoSaMP	15.63	0.57632	19.6994
DCT-II	HTP	15.63	0.66668	23.2074
DCT-II	IHT	15.63	0.66651	23.1992
DCT-II	OMP	31.5	**0.88170**	**28.6785**
DCT-II	CoSaMP	31.5	0.70914	23.2360
DCT-II	HTP	31.5	0.71074	24.4908
DCT-II	IHT	31.5	0.71047	24.4806
DCT-II	OMP	50	**0.95891**	**32.5981**
DCT-II	CoSaMP	50	0.80196	25.1387
DCT-II	HTP	50	0.81063	25.9815
DCT-II	IHT	50	0.81009	25.9670

In Fig. 2, recovered images keeping the 15.6% of the transform coefficients exhibit blocks artifacts at the edges. The recovered image using the CoSaMP presents the dark points as in the case of the Fig. 1(b). In the recovered images keeping 50% of the transform coefficients OMP does not exhibit block artifacts in the edges as the rest of the methods. However, CoSaMP, HTP and IHT methods show less speckle noise in smooth regions.

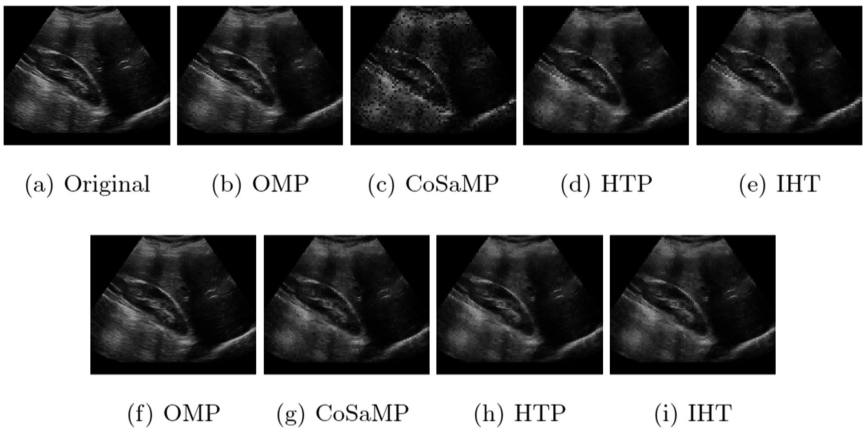

Fig. 2. Measured US data (a) original image and reconstructed images with k = 4 and 15.6% of coefficients using (b) OMP, (c) CoSaMP, (d) HTP, (e) IHT, and k = 15 and 50% of coefficients using (f) OMP, (g) CoSaMP, (h) HTP and (i) IHT.

6 Conclusions

In this study, we compared four algorithms for the reconstruction of signals with CS applied to US images. The comparisons were made on a cyst phantom and using the SSIM and PSNR metrics. The discrete cosine transform was used to find the sparse representation of the image. The results showed that the OMP algorithm has a better performance in terms of PSNR and SSIM compared to the other algorithms in the greedy search classification. Therefore, to maintain a good image quality with fewer samples than the required using the Shannon/Nyquist theorem, the OMP results the best option algorithm.

References

1. Herrick, J.F., Krusen, F.H.: Ultrasound and medicine (a survey of experimental studies). In: Transactions of the IRE Professional Group on Ultrasonic Engineering, vol. PGUE-1, pp. 4–13 (1954)
2. Donoho, D.L.: Compressed sensing. Stanford University, Technical report (2004)
3. Candes, E.J., Romberg, J., Tao, T.: Robust uncertainty principles: exact signal reconstruction from highly incomplete frequency information. Technical report (2004)
4. Lustig, M., Donoho, D.L., Santos, J.M., Pauly, J.M.: Compressed sensing MRI. IEEE Signal Process. Mag. **25**(2), 72–82 (2008)
5. Shannon, C.E.: Communication in the presence of noise. Proc. IRE **37**(1), 10–21 (1949)
6. Nyquist, H.: Certain topics in telegraph transmission theory. Trans. Am. Inst. Electr. Eng. **47** (2), 617–644 (1928)
7. Donoho, D.L.: Compressed sensing. IEEE Trans. Inf. Theory **52**(4), 1289–1306 (2006)
8. Candes, E.J., Romberg, J., Tao, T.: Robust uncertainty principles: exact signal reconstruction from highly incomplete frequency information. IEEE Trans. Inf. Theory **52**(2), 489–509 (2006)
9. Tropp, J.A., Wright, S.J.: Computational methods for sparse solution of linear inverse problems. Proc. IEEE **98**(6), 948–958 (2010)
10. Tropp, J.A., Gilbert, A.C.: Signal recovery from random measurements via orthogonal matching pursuit. IEEE Trans. Inf. Theor. **53**(12), 4655–4666 (2007)
11. Needell, D., Tropp, J.A.: CoSaMP: iterative signal recovery from incomplete and inaccurate samples. Appl. Comput. Harmonic Anal. **26**(3), 301–321 (2009)
12. Foucart, S.: Hard thresholding pursuit: an algorithm for compressive sensing. SIAM J. Numer. Anal. **49**(6), 2543–2563 (2011)
13. Blumensath, T., Davies, M.E.: Iterative hard thresholding for compressed sensing. Appl. Comput. Harmonic Anal. **27**(3), 265–274 (2009)
14. Candes, E.J., Wakin, M.B.: An introduction to compressive sampling. IEEE Signal Process. Mag. **25**(2), 21–30 (2008)
15. Natarajan, B.K.: Sparse approximate solutions to linear systems. SIAM J. Comput. **24**(2), 227–234 (1995)
16. Mallat, S.G., Zhang, Z.: Matching pursuits with time-frequency dictionaries. IEEE Trans. Signal Process. **41**(12), 3397–3415 (1993)
17. Liu, L., Xie, Z., Feng, J.: Backtracking-based iterative regularization method for image compressive sensing recovery. Algorithms **10**(1), 7 (2017)

18. Bouchot, J.L., Foucart, S., Hitczenko, P.: Hard thresholding pursuit algorithms: number of iterations. Appl. Comput. Harmonic Anal. **41**(2), 412–435 (2016)
19. Foucart, S., Rauhut, H.: A Mathematical Introduction to Compressive Sensing. Birkhauser, Cambridge (2013)
20. Jensen, J.A.: Field II simulation program. https://field-ii.dk/